Talanta 110 (2013) 96–100

Contents lists available at SciVerse ScienceDirect

Talanta

journal homepage: www.elsevier.com/locate/talanta

Bienzymatic glucose biosensor based on direct electrochemistry of cytochrome *c* on gold nanoparticles/polyaniline nanospheres composite

Cuili Xiang [a], Yongjin Zou [a], Shujun Qiu [a], Lixian Sun [a,b,*], Fen Xu [a,c,*], Huaiying Zhou [a]

[a] Guangxi Key Laboratory of Information Materials, Guilin University of Electronic Technology, Guilin 541004, PR China
[b] Dalian Institute of Chemical Physics, Chinese Academy of Sciences, Dalian 116023, PR China
[c] Department of Chemistry and Chemical Engineering, Liaoning Normal University, Dalian 116029, PR China

ARTICLE INFO

Article history:
Received 1 December 2012
Received in revised form
2 February 2013
Accepted 8 February 2013
Available online 20 February 2013

Keywords:
Cytochrome *c*
Gold nanoparticles
Polyaniline nanoshpere
Direct electron transfer
Glucose biosensor

ABSTRACT

Gold nanoparticles (GNPs) assembled polyaniline nanospheres (PANS) composite were prepared by noncovalent strategy. Cytochrome *c* (Cyt *c*) was electrostatically adsorbed on the GNPs/PANS modified electrode. The direct electron transfer (DET) between Cyt *c* and GNPs/PANS modified electrode was investigated. Cyt *c* shows a couple of quasi-reversible and well-defined cyclic voltammetry (CV) peaks with a formal potential ($E^{0'}$) of −0.27 V (versus Ag/AgCl) in pH 7.0 phosphate buffer solution (PBS). The Cyt *c*/GNPs/PANS modified electrode gives an improved electrocatalytic activity toward the reduction of hydrogen peroxide (H_2O_2). The catalysis currents increase linearly to the H_2O_2 concentration in a wide range of 0.01–2.4 mM with a correlation coefficient 0.998. After immobilized glucose oxidase (GOD) on the Cyt *c*/GNPs/PANS modified electrode by Nafion polymer, a bienzymatic glucose biosensor was further prepared for sensitive detection of glucose. The amperometric detection of glucose was assayed by potentiostating the bienzymatic electrode at −0.2 V versus Ag/AgCl to reduce the enzymatically produced H_2O_2 with minimal interference from the coexisting electroactive compounds. The proposed glucose biosensor exhibits good response performance to glucose with a wide linear range from 0.01 to 3.2 mM with a correlation coefficient of 0.997. The electrode has high sensitivity of 63.1 μA mM^{-1} cm^{-2} and a detection limit 0.01 mM at the signal-to-noise ratio of 3. Moreover, the glucose biosensor possesses good stability and reproducibility.

1. Introduction

During recent years, direct electron transfer (DET) between proteins and electrodes has been widely investigated due to its broad application in many areas. Understanding the electron transfer between proteins and electrode can provide deep insight into physiological processes as well as impetus for the further development of amperometric biosensors and bioelectrocatalytic systems [1,2]. Among these proteins, the study of direct electron transfer between cytochrome *c* (Cyt *c*) and electrode has gained increasing attention [3–5]. Cyt *c* plays an important role in the biological respiratory chain, whose function is to receive electrons from Cyt *c* reductase and deliver them to Cyt oxidase. However, it is difficult for Cyt *c* to exhibit a voltammetric response at a bare electrode, most probably due to protein denaturation at the bare electrode surface leading to extremely slow electron transfer kinetics or in the light of its three dimensional structure which hinders interaction with the electrode [6].

Recently, nanomaterials are widely used to realize the direct electrochemistry of Cyt *c*, as they have large surface area, good biocompatibility and/or conductivity, which can facilitate the electron transfer between enzyme and the underlying electrodes [7–10]. In particular, conducting polymer, which are a new type of nanomaterials, have been extensively studied for the fabrication of new classes of advanced materials because of their remarkable electronic and biocompatible properties combined with high chemical stability. Furthermore, conducting polymer modified electrode has been demonstrated to promote electron-transfer reactions between enzyme and the electrode surfaces [10–12].

On the other hand, gold nanoparticles (GNPs), due to its good biocompatibility, excellent electronic conductivity and relatively large surface area, have been widely used in modification of various electrodes and fabrication of different kinds of biosensors. GNPs have been attached on the multiple substrate by various methods [13,14], but these methods seem to be tedious and complex. Moreover, few reports focus on decorating gold nanoparticles onto nanostructured conducting polymer. Polyaniline is considered as one of the most attractive conducting polymer due to its unique electrochemical

* Corresponding authors at: Guangxi Key Laboratory of Information Materials, Guilin University of Electronic Technology, Guilin 541004, China. Fax: 86-773-2191903.
E-mail addresses: lxsun@dicp.ac.cn (L. Sun), fenxu@dicp.ac.cn (F. Xu).

0039-9140/$ - see front matter © 2013 Elsevier B.V. All rights reserved.
http://dx.doi.org/10.1016/j.talanta.2013.02.022

properties, facile synthesis, and excellent conductivity, high environmental stability and biocompatibility. In the present paper, GNPs assembled polyaniline nanospheres (PANS) was fabricated in a simple and robust way. The nanocomposite shows good affinity to immobilize proteins. Cyt *c* was successfully immobilized on the GNPs/PANS modified electrode by the electrostatically adsorbed method. The prepared electrode shows improved direct electrochemical behaviors of Cyt *c* and displays excellent electrocatalytical responses to the reduction of H_2O_2. After immobilized glucose oxidase (GOD) with Nafion polymer on the electrode, a bienzymatic glucose biosensor was further prepared for highly selective and sensitive detection of glucose. Operational characteristics of the bienzymatic sensor, in terms of linear range, detection limit, sensitivity, selectivity and stability were presented in detail. The proposed glucose biosensor is promising for practical usage due to its excellent analytical performance. And also this work provides a new platform for fabricating biosensor based on oxidase.

2. Experimental

2.1. Reagents

Horse heart cytochrome *c* (MW 12,384) was purchased from Sigma and used without further purification. Aniline monomer, Ammonium persulfate (APS), cellulose acetate, $HAuCl_4 \cdot 3H_2O$ were obtained from Sinopharm Chemical Reagent Co., Ltd. (Shanghai, China). GOD (from *Aspergillus niger*; 300,000 unit g^{-1}) was purchased from Sanland (America). D-glucose was used without further purification and glucose solutions were stored overnight at room temperature before use. All other chemicals from commercial source were of analytical grade and used as received. 0.1 M phosphate buffer solution (PBS), which was made from Na_2HPO_4 and NaH_2PO_4, was employed as supporting electrolyte. Deionized water was used throughout the experiments.

2.2. Apparatus and measurements

All electrochemical measurements were performed on an IM6e electrochemical workstation (Zahner-Elektrik, Kronach, Germany). The working electrode was the Bioanalytical Systems (BAS) cavity glass carbon (GC) electrode (3 mm diameter). The rotating disk electrode experiments were performed by the BAS rotator system in conjunction with an IM6e. The rotating rate is 4000 rpm when detect H_2O_2 and glucose. An Ag/AgCl (saturated with NaCl) reference electrode was used for all measurements. A platinum wire was used as a counter electrode. Before all batch amperometric experiments, the potential of each electrode was held at the operating value, allowing the background current to decay to a steady state value.

Electrochemical impedance spectroscopy (EIS) measurements were performed in the presence of 5 mM $K_3[Fe(CN)_6]/K_4[Fe(CN)_6]$ (1:1) and 0.1 M KCl by applying an alternating current voltage with 5 mV amplitude in a frequency range from 0.1 Hz to 100 kHz. The electrolyte solution was purged with high-purity nitrogen for 15 min prior to electrochemical experiments and a nitrogen environment was then maintained for the solution during the measurement process except the amperometric experiments for the bienzymatic glucose biosensor. All experiments were performed at room temperature (20 ± 1 °C).

Transmission electron microscope (TEM) images were obtained from a JEM-2000EX microscope (Japan).

2.3. Preparation of GNPs/PANS composite

GNPs were prepared by reduction of $HAuCl_4 \cdot 3H_2O$ in aqueous solution according to reference [15]. The average nanoparticle diameter is about 10 nm (data not shown). PANS were prepared by chemical oxidation of aniline monomer in acetone solution according to the established procedures [16]. Briefly, 2.5 mL acetone, 0.8 mL dimethylacetamide, and 0.4 g cellulose acetate were mixed together with magnetic stirring at room temperature. After 3 h, aniline (0.08 mL) was added into the above solution and stirred for 1 h. Then, 1 g oxalic acid and 2 g APS were added to the mixture and the magnetic stirring was kept for 2 h. The final solution was kept in refrigerator at 4 °C for 48 h. Sequentially, the mixture was soaked with acetone under stirring for 10 min. The product was centrifuged and rinsed thoroughly with water and methanol to remove the residual monomers, oxidants and their decomposition products. Then the product was dispersed in water at a concentration of 10 mg mL^{-1} with the aid of ultrasonication for 30 min. GNPs assembled PANS was prepared by adding 50 mL GNPs solution into 10 mL of 10 mg mL^{-1} PANS nanospheres suspension. The precipitated GNPs/PANS nanospheres were centrifuged and washed with water several times. Finally, the composite was dried in vacuum for 12 h prior to use.

2.4. Fabrication of the modified electrodes

1 mg of GNPs/PANS composite was dispersed in 2 mL water with the aid of ultrasonic bath to give a 0.5 mg mL^{-1} black suspension. The GC (3 mm in diameter) electrode was polished carefully with 1.0, 0.3 and 0.05 μm alumina slurry, and then utrasonicated successively in 1:1 nitric acid, acetone and deionized water, respectively. After dried at room temperature, a suspension (10 μL) of the GNPs/PANS was dropped on the GC electrode and then dried under an infrared lamp. After thoroughly rinsed with water, the obtained electrode was immersed in the 2 mg/mL Cyt *c* solution for 10 h at 4 °C.

GOD solution was obtained by dissolving 10 mg of GOD in 2 mL of 0.1 M PBS (pH 7). For the preparation of the glucose biosensor, 3 μL of GOD solution was dropped onto the Cyt *c*/GNPs/PANS modified electrode surface carefully. After drying for 1 h at room temperature, a 1% (3 μL) Nafion solution was placed on the enzyme surface as protective film. The reaction process of the bienzyme electrode is illustrated in Scheme 1.

3. Results and discussion

3.1. Characterization of the modified GC

The morphologies of the as-prepared PANS and GNPs/PANS were studied by means of TEM. As shown in Fig. 1, PANS are uniform with average diameter in the range of 90–120 nm. Most of the nanospheres were in the form of aggregations, which could

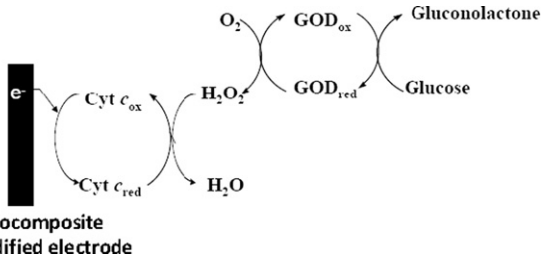

Scheme 1. The reaction illustration of the GOD/Cyt *c*/GNPs/PANS/GC bienzyme electrode.

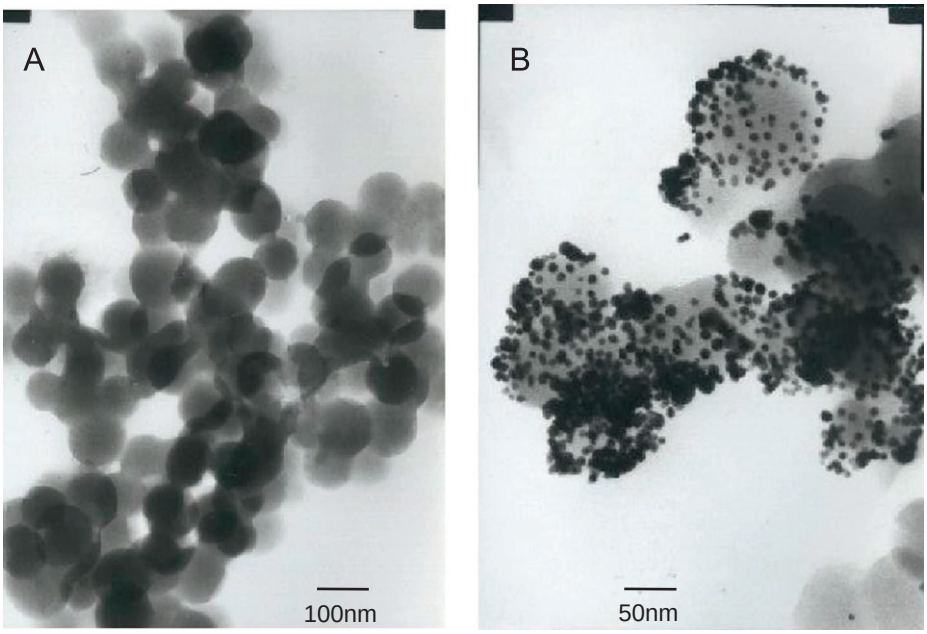

Fig. 1. TEM images of polyaniline nanospheres (A) and GNPs/polyaniline nanospheres composite (B).

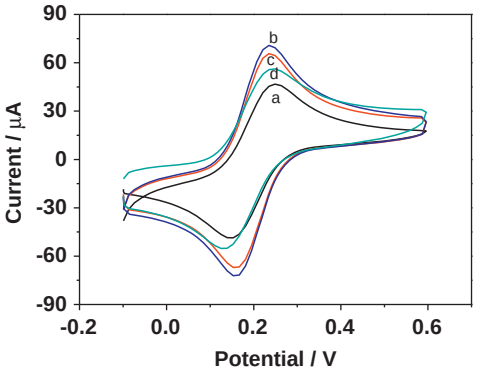

Fig. 2. CVs at (a) GC, (b) PANS/GC, (c) GNPs/PANS/GC, and (d) Cyt c GNPs/PANS/GC electrodes in 0.1 M KCl and 5 mM $Fe(CN)_6^{3-/4-}$ solution, scan rate, 50 mV s^{-1}.

benefit the sensor performance because the well-dispersed PANS were electrochemical accessible. A direct evidence for the attachment of GNPs on the PANS was showed in Fig. 1b. The GNPs with high density were well dispersed on the surface of the PANS, which provide a good biocompatible interface and excellent microenvironment for the immobilization of proteins. Interestingly, the density of the decorated GNPs was found to be controllable by change the ratio (volume of GNPs solution versus volume PANS suspension) of GNPs and PANS. Under the optimized condition, the ratio of 5 was chosen to prepare the biosensor in the present paper.

Cyclic voltammetry (CV) and EIS were used to characterize the modification of the electrode in 5 mM $Fe(CN)_6^{3-/4-}$ and 0.1 M KCl solution. Fig. 2 compares the CVs response at GC, PANS/GC, GNPs/PANS/GC, Cyt *c*/GNPs/PANS/GC electrodes in the above solution. Compared with bared GC electrode, the anodic and cathodic peak currents on the PANS modified electrode are increased (curve b), indicating PANS improves the surface area of electrode substantially. When GNPs are assembled on the surface of PANS, the peak currents decrease a little but still much higher than that at GC electrode (curve c). It maybe attribute to the distribution of GNPs with negative charge on surface of PANS to hinder the diffusion of ferricyanide toward the electrode surface, which is similar to the reference [17]. After immobilizing Cyt *c* on the GNPs/PANS/GC electrode, the peak currents dropped again. It may attribute that protein is nonconductive and hinder the electron transfer. The capability of electron transfer on the modified electrode was also investigated by EIS (Fig. S1). At the naked GC electrode, the electron transfer resistance (R_{et}) can be estimated to be 460 Ω (curve a). After coated with PANS and GNPs/PANS films, the R_{et} decreases dramatically, nearly to zero at curves b and c, indicating that the PANS and GNPs/PANS form high electron conduction pathways between the electrode and electrolyte, and obviously improve the diffusion of ferricyanide toward the electrode surface. These results were consistent with the CV tests. An obvious increase in the interfacial resistance is observed when the heme protein Cyt *c* was immobilized on GNPs/PANS/GC electrode (curves d) (Table S1), resulting from the hindered pathway of electron transfer by Cyt *c*. These results indicated that Cyt *c* was successfully immobilized on the surface of the modified electrode.

3.2. DET of Cyt c on the Cyt c/GNPs/PANS/GC electrode

Direct electron transfer (DET) of Cyt *c* on the GNPs/PANS modified electrode was examined by voltammetry. The CVs of different modified electrodes were obtained in 0.1 M PBS (pH 7.0) at a scan rate 100 mV/s. To study the electrochemical response of the Cyt *c* on the bare GC electrode, the GC electrode was inserted in the 0.5 mg mL^{-1} Cyt *c* solution directly. As shown in Fig. 3, no obvious redox peaks can be observed at the Cyt *c*/GC electrode in the potential range from −0.7 to 0.3 V (curve a). A pair of well-defined and quasi-reversible redox peaks was shown on the Cyt *c*/GNPs/PANS/GC and Cyt *c*/PANS/GC modified electrode, corresponding to the electrochemical redox reaction between Cyt *c*-Fe(III) and Cyt *c*-Fe(II). These results indicated that DET has been achieved between the Cyt *c* heme protein and the PANS-based modified electrode. But the peak current on the Cyt *c*/GNPs/PANS/GC electrode is higher than that of Cyt *c*/PANS/GC modified electrode obviously, indicating that GNPs/PANS is a more effective matrix than PANS to realize the DET of Cyt *c*. The anodic peak potential (E_{pa}) and cathodic peak potential (E_{pc}) were located at −0.221 and −0.307 V on the Cyt *c*/GNPs/PANS/GC electrode,

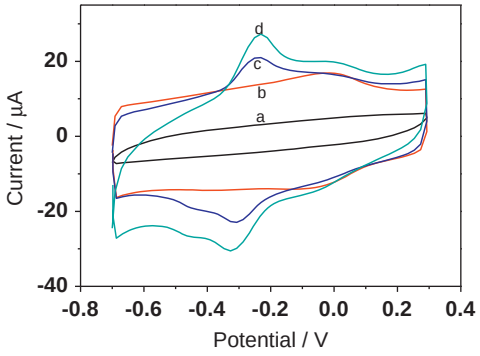

Fig. 3. CVs at: (a) Cyt c/GC, (b) PANS/GC, (c) Cyt c/PANS/GC, and (d) Cyt c/GNPs/PANS/GC electrodes in pH 7.0 PBS; scan rate, 100 mV s^{-1}.

respectively. The formal potential ($E^{0'}$) taken by the average value of the anodic and cathodic peak potential was ca. −0.26 V and the peak-to-peak separation (ΔE_p) was 75 mV at the scan rate of 100 mV/s, indicating a fast electron transfer reaction. These results reveal that the DET of Cyt *c* has been realized on the Cyt *c*/GNPs/PANS/GC modified electrode. To examine the stability of the Cyt *c* immobilization on the nanocomposite, Cyt *c*/GNPs/PANS/GC modified electrode was immersed into PBS solution and CV curves were recorded (Fig. S2). There is no obvious peak decrease after 50 cycles, which indicates the immobilization of Cyt *c* on the electrode is quite good.

The cyclic voltammograms of Cyt *c*/GNPs/PANS/GC electrode in pH 7.0 PBS at different scan rates was also investigated (Fig. S3). Both the cathodic and anodic peaks currents are linearly proportional to the scan rate in the wide range from 100 to 900 mV/s, which indicate that the electrode reaction corresponds to a surface-controlled quasi-reversible process. Meanwhile, the peak-to-peak separation increases with the increase of scan rate. An estimation of the electron transfer rate constant (k_s) has been made from the peak potential separation value using the model of Laviron [18] for a surface-controlled electrode process. The electron transfer rate constant can be estimated to be 2.362 s^{-1}. It was much higher than that of Cyt *c* adsorbed in graphene-based modified electrode (1.95 s^{-1}) [4], ordered mesoporous niobium oxide film (0.28 s^{-1}) [19] and NaY zeolite (0.78 ± 0.04 s^{-1}) [20]. The fast k_s indicates that the GNPs/PANS composite film was an excellent promoter for the electron transfer between Cyt *c* and the electrode.

3.3. Electrocatalysis of Cyt c/GNPs/PANS/GC electrode

In order to explore the electrocatalytic activity of the Cyt *c*/GNPs/PANS/GC modified electrode, its response toward the reduction of H_2O_2 was studied (Fig. S4). After the addition of H_2O_2, the electrochemical behavior of Cyt *c* immobilized electrode changes dramatically. The reduction peak current increases obviously, while the oxidation peak current decreases with increasing the concentration of H_2O_2, showing a typical electrocatalytic reduction process of H_2O_2. These results demonstrate that Cyt *c*/GNPs/PANS/GC has a good catalytic activity toward H_2O_2.

The capability of the enzymatic electrode can be enlisted for the detection of H_2O_2. Fig. 4 shows a typical current–time plot of the Cyt *c*/GNPs/PANS/GC electrode upon the successive addition of 0.1 mM H_2O_2. Based on the optimal experiments, −0.2 V was selected as the applied potential. As shown in Fig. 4, the reductive current increases to reach 95% of the steady state current within 5 s, suggesting the response of the electrode to H_2O_2 should be a quick responsive process. The linear range of H_2O_2 was from 0.01 to 2.4 mM with a correlation coefficient of 0.998 (Fig. 4, inset), a

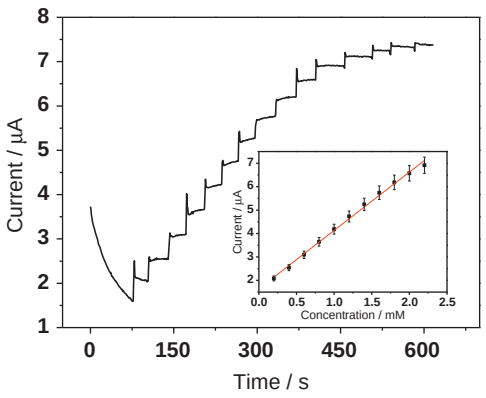

Fig. 4. Amperometric responses of the Cyt c modified electrodes at –0.20 V upon successive additions of 0.2 mM H_2O_2 to 10 mL PBS (0.1 M, pH 7.0). rotating rate, 4000 rpm. Inset: The calibration curve of the H_2O_2 biosensor.

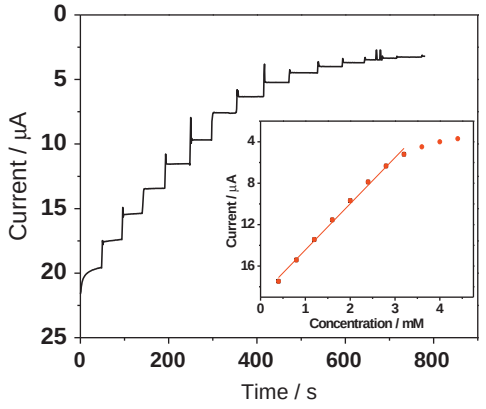

Fig. 5. Typical current–time plot for the biosensor upon the successive addition of 0.4 mM glucose at −0.2 V in 0.1 M pH 7.0 PBS, rotating rate, 4000 rpm. Inset: calibration curve of the biosensor as a function of glucose concentrations.

detection limit of 0.003 mM was estimated at the signal-to-noise ratio of 3. The modified electrode displays a wider linear range and lower detection limit than those reported in literature [21]. The excellent electrocatalytic activity of the electrode toward H_2O_2 also means that the electrode can represent a new electrochemical platform that provides operational access to a large number of oxidase-based enzymes for fabricating bienzyme biosensors.

3.4. Amperometric determination of glucose at the bienzymetic electrode

Due to the fast DET between Cyt *c* and GNPs/PANS composite and rapid response of Cyt *c*/GNPs/PANS/GC toward H_2O_2, a bienzymatic electrode was further constructed for the sensitive detection of glucose. Fig. 5 shows a typical current–time plot for the enzyme electrode upon the successive addition of 0.2 mM glucose at −0.2 V. The current response of the enzyme electrode decreased along with glucose concentration. This is attributed to the electrocatalytic response to dissolved oxygen, which is similar to the literature [22]. Based on the decrease of the electrocatalytic response to dissolved oxygen, this system can be used as a glucose biosensor. The modified electrode reached 95% of the steady state current within 5 s. The calibration curve is shown in Fig. 5 (inset). The enzyme electrode gave a linear response to glucose in the range from 0.01 to 3.2 mM with a correlation coefficient of 0.997. The electrode has high sensitivity of 63.1 μA mM^{-1} cm^{-2} and a detection limit 0.01 mM at the

signal-to-noise ratio of 3. The sensitivity of the resulting biosensor is much higher than the reported 29.9 μA mM^{-1} cm^{-2} [23],0.98 μA mM^{-1} cm^{-2} [24] and 9.9 μA mM^{-1} cm^{-2} [25]. The bienzyme biosensor has high sensitivity due to chemical amplification, which is rapidly increased by the rise in enzymatic activity [26]. It indicates that the immobilizing process may retain the good enzymatic activity.

3.5. Performance of the glucose biosensor

The interference of electroactive species on glucose detection and selectivity of the glucose biosensor was evaluated. The most common electrochemical interfering species, such as ascorbic acid and acetaminophen were examined. Addition of 0.2 mM ascorbic acid, 0.2 mM acetaminophen to 0.5 mM glucose did not produce observable interference in the biosensor response. These results indicate the glucose biosensor has high selectivity, which may be due to the low potential applied. Futhermore, Nafion polymer, a perselective barrier, can circumvent the entry of anionic biological interferences effectively.

The reproducibility of enzyme electrode construction was estimated from the response to 0.5 mM glucose at five enzyme electrodes prepared under the same conditions (Fig. S5). The results revealed that the biosensor has a satisfied reproducibility with a relative standard deviations (RSD) of 4.6%. The operational stability of the enzyme electrode was measured at 0.0 V in 0.10 M PBS+0.1 M KCl containing 0.5 mM glucose (Fig. S6). Less than 2.4% relative deviation was obtained for five times continuous determinations of the same sample, which indicates that the biosensor has a good operational stability. Excellent reproducibility seems to mean that little amount enzyme was leaked out from the electrode surface which indicated the immobilizing method of enzyme was effective.

To evaluate the practical usage of the glucose biosensor, a series of human serum samples were tested (Table S2). The values measured by the present system and hospital are very close. The RSD for five samples are less than 5%, which indicates the glucose biosensor is reliable for practical application.

The storage stability of the biosensor was also studied. The steady-state response current of 0.5 mM glucose was determined every 2 days. When not in use, the biosensor was stored dry at 4 °C (Fig. S7). The results show that the steady-state response current only decreases by 8% after 30 days (15 times) measurements, which indicates that the enzyme electrode was considerably stable. The good stability of the biosensor can be attributed that GNPs/PANS can form strong interaction between the enzymes and maintain the activity of the enzyme favorably.

4. Conclusions

An easy and effective method for fabricating GNPs/PANS modified GC electrode was developed in the present paper. The direct electron transfer of Cyt *c* on the modified electrode was achieved. The results show that the GNPs/PANS composite film can promote the direct electron transfer between the redox proteins and the underlying electrode and keep the activity of the enzyme well. The Cyt *c*/GNPs/PANS modified electrode as a biosensor for the catalytic reduction of H_2O_2 was also investigated. The results show that the GNPs/PANS composite film was an excellent matrix for studying the direct electrochemistry of protein and fabricating biosensor. Based on these, a bienzymatic glucose biosensor was further prepared. The glucose biosensor also shows excellent analytical performance. The nanocomposites provide a new electrochemical platform for designing a variety of bioelectrochemical devices.

Acknowledgments

The authors wish to express their gratitude and appreciation for the financial support from the initial foundation of Guilin University of Electronic Technology (UF11024Y), Guangxi Key Laboratory of Information Materials (PF12001X and PF12003X), the National Science Foundation of China (20833009, 51071146, 51071081, 21173111, 51201041, and 51201042), and the NSFCGX (2012GXNSFGA060002).

Appendix A. Supporting information

Supplementary data associated with this article can be found in the online version at http://dx.doi.org/10.1016/j.talanta.2013.02.022.

References

[1] M. Wang, Q. Sheng, D. Zhang, Y. He, J. Zheng, Bioelectrochemistry 86 (2012) 46–53.
[2] J. Li, J. Tang, L. Zhou, X. Han, H. Liu, Bioelectrochemistry 86 (2012) 60–66.
[3] F. Schroper, A. Baumann, A. Offenhausser, D. Mayer, Biosens. Bioelectron. 34 (2012) 171–177.
[4] J.F. Wu, M.Q. Xu, G.C. Zhao, Electrochem. Commun. 12 (2010) 175–177.
[5] C. Mu, Q. Zhao, D. Xu, Q. Zhuang, Y. Shao, J. Phys. Chem. B 111 (2007) 1491–1495.
[6] J.J. Feng, G. Zhao, J.J. Xu, H.Y. Chen, Anal. Biochem. 342 (2005) 280–286.
[7] Y.L. Zhou, H.S. Yin, X.M. Meng, Z.N. Xu, Y.R. Fu, S.Y. Ai, Eelectrochim. Acta 71 (2012) 294–301.
[8] J. Wang, Microchim. Acta 177 (2012) 3–4.
[9] C.C. Guo, H. Sun, X.S. Zhao, Sens. Actuator. B 164 (2012) 84–89.
[10] X.Y. He, L. Zhou, E.P. Nesterenko, P.N. Nesterenko, B. Paull, J.O. Omamogho, J.D. Glennon, J.H.T. Luong, Anal. Chem. 84 (2012) 2351–2357.
[11] X.L. Xiao, B. Zhou, L. Zhu, L.L. Xu, L. Tan, H. Tang, Y.Y. Zhang, Q.J. Xie, S.Z. Yao, Sens. Actuator. B 165 (2012) 126–132.
[12] X.J. Chen, Z.X. Chen, J.W. Zhu, C.B. Xu, W. Yan, C. Yao, Bioelectrochemistry 82 (2011) 87–94.
[13] J. Njagi, S. Andreescu, Biosen. Bioelectron. 23 (2007) 168–175.
[14] U.S. Mohanty, J. Appl. Electrochem. 41 (2011) 257–270.
[15] K.C. Grabar, K.J. Allison, B.E. Baker, R.M. Bright, K.R. Brown, R.G. Freenman, A.P. Fox, C.D. Keating, M.D. Musick, M.J. Natan, Langmuir 12 (1996) 2353–2361.
[16] Y. Zou, J. Pisciotta, I.V. Baskakov, Bioelectrochemistry 79 (2010) 50–56.
[17] C. Xiang, Y. Zou, L. Sun, F. Xu, Talanta 74 (2007) 206–211.
[18] E. Laviron, J. Electroanal. Chem. 100 (1979) 263–270.
[19] X. Xu, B. Tian, J. Kong, S. Zhang, B. Liu, D. Zhao, Adv. Mater. 15 (2003) 1932–1936.
[20] Z. Dai, S. Liu, H. Ju, Electrochim. Acta 49 (2004) 2139–2144.
[21] H.S. Yin, S.Y. Ai, W.J. Shi, L.S. Zhu, Sens. Actuator. B 137 (2009) 747–753.
[22] S. Wu, H. Ju, Y. Liu, Adv. Funct. Mater. 17 (2007) 585–592.
[23] S. Hrapovic, Y. Liu, K.B. Male, H. John, T. Luong, Anal. Chem. 76 (2004) 1083–1088.
[24] M. Yang, Y. Yang, H. Yang, G. Shen, R. Yu, Biomaterials 27 (2006) 246–255.
[25] J. Li, X. Lin, Biosens. Bioelectron. 22 (2007) 2898–2905.
[26] J.J. Kulys, Enzym. Microb. Technol 3 (1981) 344–352.